# Improving the fine scale rainfall estimation of a local area weather radar: case of an X-band radar at Leuven, Belgium


Decloedt Laurens Cas

Laurens Cas Decloedt[1], J. Van Assel[2], P. Willems[1]
*1 Hydraulics Laboratory - KU Leuven, Kasteelpark 40, 3001 Heverlee, Belgium,*
*Cas.Decloedt@bwk.kuleuven.be or Patrick.Willems@bwk.kuleuven.be*
*2 Aquafin, Dijkstraat 8, 2630 Aartselaar, Belgium, Johan.Vanassel@aquafin.be*
(Dated: 04 June 2012)

## 1. Introduction

Observational rainfall data is used for a wide range of applications, such as the design and operational management of sewer systems. The rainfall input data should be as accurate as possible, preferably describing the spatial variability as well. With a network of rain gauges, it is very expensive to get a good insight in the spatial structure of rainfall fields. This is where radar rainfall measurements come into the picture. A previous study (Goormans, 2011) investigated whether a certain type of short-range, cost-effective, high resolution local weather radar, the Local Area Weather Radar - City model (LAWR-CR, DHI), could be a valuable asset in providing rainfall input data to a sewer model.

The LAWR-CR was installed at the city of Leuven, Belgium, and the sewer system of Winksele-Herent-Wijgmaal (WHW, close to Leuven) was considered as sewer system case study (Figure 1). The radar data require adjustments to obtain a higher accuracy of local rainfall intensities. Those adjustments were based on tipping bucket rain gauge measurements. Various correction methods were applied and compared. The impacts of a large number of rainfall events on the sewer system of WHW were simulated and the effect of different types of radar based rainfall input on the model results investigated. Large quantitative deviations were found between flow observations in the sewer pipes and the LAWR-CR driven simulations. However, the qualitative course of water depth and flow variations in the monitored conduits was reproduced fairly well.

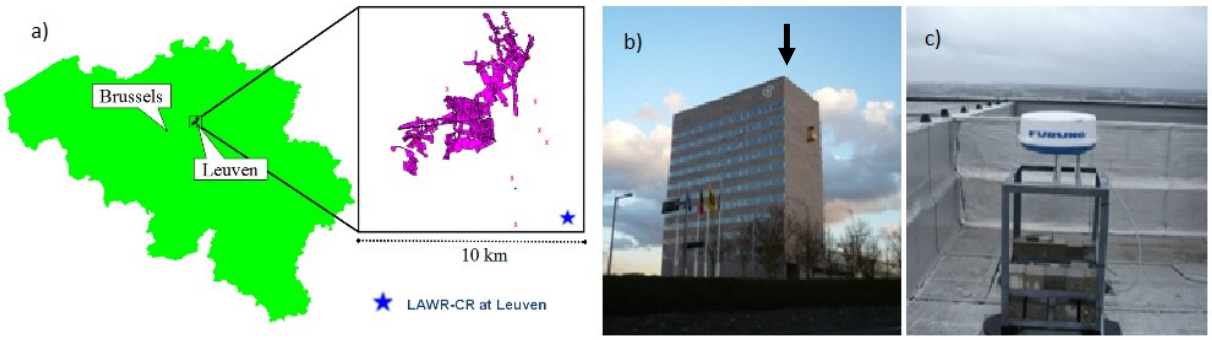


*Figure 1: a) Location of Leuven in Belgium and the location of the LAWR-CR relative to the WHW sewer network, b) the LAWR-CR installation site: the Provinciehuis building and c) the city-LAWR on the rooftop (with the wall as a clutter fence)*

## 2. Objectives and methodology

Further improvements are being made to the LAWR-CR based fine scale rainfall estimates in order to make these useful for the design of new urban sewer systems and the management of existing infrastructure. This is done based on new adjustment methods that account for more influential variables such as the duration of the rainfall event, the size of the rainfall field, the cloud movement speed and direction, etc. A convective - stratiform separation algorithm (based on Steiner et al. 1995) has also been implemented and adapted for this local scale application.

### 2.1. Radar and gauge network specifications

The City-LAWR (LAWR-CR) is a short range X-band radar based on marine radar technology (Furuno 1834 model). The specifications are given in Table 1 and compared to the normal LAWR. The radar is not able to scan at different elevation levels, produce 3D images or measure radial velocities of the particles (DHI (2010); Goormans (2011)).

The LAWR-CR does not measure reflectivity in [dBZ] as usual radars do, since it is based on marine X band technology. The measurements are produced in DRO (Dimensionless Radar Output) and are expressed in ‘counts’ per minute, depending on the strength of the returning signal. This number of counts can then be ‘calibrated’ or adjusted to rainfall intensities.

Since the LAWR has a rather high vertical opening angle (20°), the lower part of the beam deflects towards the ground and gives a false signal (ground clutter). To reduce the amount of clutter, use is made of the wall surrounding the LAWR-CR as a clutter fence (Figure 1). In this way, the lower half of the radar beam is cut off by absorbing the incoming electromagnetic energy or deflecting the waves away from the radar receiver, while leaving the upper part of the radar beam untouched. Figure 2 shows that the Leuven LAWR-CR images have a blanked sector, because no radar scanning permission was obtained for the direction of the Brussels Airport due to possible interference with the airport navigation system.

*Table 1: specifications of the LAWR and City-LAWR*

| Parameter | LAWR | City-LAWR |
|---|---|---|
| Peak Power | 25 kW | 4 kW |
| Frequency / Band | 9.41 GHz ± 30MHz / X-band | |
| Wave / Bin length | 3.2 cm / 120 m | |
| Pulse length | 0.8-1.2 µs | 0.8 µs |
| Antenna unit | 2.5 m slotted waveguide array | 0.4 m radome |
| Receiver | Logarithmic receiver | |
| Vertical opening angle | ± 10° from horizontal (20° in total) | |
| Horizontal opening angle | 0.95° | 4° |
| Samples pr. rotation | 360 | 450 |
| Range (forecast/QPE) | 60/20 km | 30/15 km |
| Spatial resolution (grid size - range) | 500x500m (60km), 250x250m (30km), 300x300m (15km), 100x100m (15km) | 250x250 m (30 km), 125x125m (15km), 150x150 m (7.5 km), 50x50m (7.5km) |
| Temporal resolution | 1 or 5 minutes (1 min in this study) | |
| Scanning strategy | Single layer and continuous scanning | |

Four tipping bucket rain gauges (TBR) are installed in and around Leuven (Table 2 and Figure 3), operated by Aquafin nv. Rainfall intensities are recorded with a time step of 2 minutes and a resolution of 0.2mm. The rain gauges have been dynamically calibrated (Goormans and Willems, 2008). The data is checked manually for inconsistencies between gauges and for differences between daily totals and intensities. Possible wrong measurements are marked.

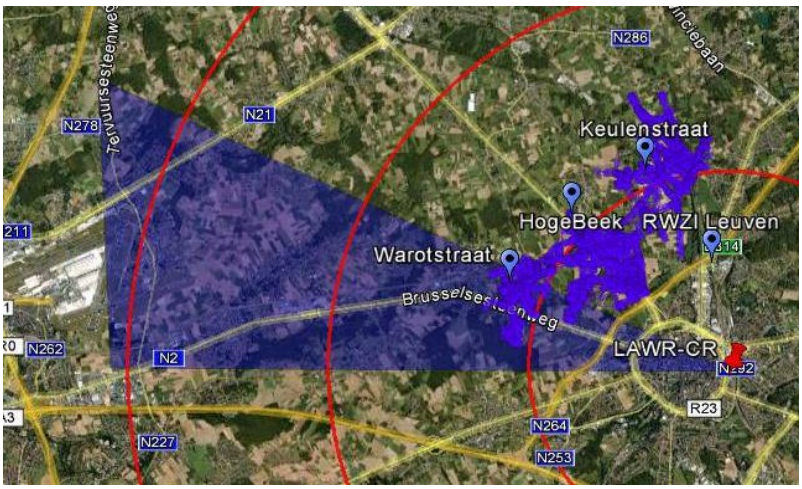


*Figure 2: Location of the rain gauges RWZI (WZ), Keulenstraat (KL), HogeBeek (HB) and Warotstraat (WS) [blue pins] relative to the LAWR-CR [red pin] (the red concentric circles have radii of 5km, 10km and 15km), the purple area is the blanked sector and the blue network is the Winksele Herent Wijgmaal (WHW) sewer network.*

*Table 2: Rain gauge network specifications*

| Name | Location | Time step | Resolution | Distance from radar |
|---|---|---|---|---|
| WZ | RWZI - Wastewater treatment plant Leuven | 2 minutes | 0.2mm | 2.51km (north) |
| HB | HogeBeek – Storm water retention basin | | | 5.74km (north-west) |
| KL | Keulenstraat – Sewer overflow structure | | | 5.85km (north) |
| WS | Warotstraat – **Not used** due to Brussels airport | | | 5.74km (north-west) |

### 2.2. Variables and algorithm specifications

In order to improve the radar adjustment based on the TBR measurements, the radar – TBR residuals were statistically analyzed. This was done for all rainfall events over the period June 2008 till October 2011 with some missing periods. The event rainfall depth (in mm; hereafter called Gaugesum) was plotted versus the sum of the radar counts (hereafter called Radarsum). The slope of a linear regression line of Gaugesum versus Radarsum, hereafter called adjustment factor, was calculated and the dependency searched between this adjustment factor and various potential explanatory variables. The variables investigated in this study consist of the duration of the event, the mean air temperature, the mean rainfall intensity (measured by the TBRs) and the relative coverage of the radar image by rainfall during the event. The seasonal variations are taken into account, as well as the convective or stratiform nature of the event and the cloud movement speed and direction during the event. To determine these last two variables, new algorithms have been designed and tested. A storm separation algorithm defines the starting and ending times of the different storm periods based on a set of criteria. Two storm events are classified as different events when each event have a storm duration longer than 20 minutes, when they are separated in time by more than 2 hours and when the accumulated rainfall depth is higher than 1mm (measured by TBR).

The coverage of the radar image by rainfall is the percentage of the radar image that contains rain, averaged over the duration of the event. The mean rainfall intensity is the mean of the rainfall intensities measured by the gauges, averaged over the duration of the event. For the mean air temperature during the event, a temperature series of the Flemish Environment Agency, was used for the mean daily air temperature at a height of 1.75m at the measuring station of Herentals (about 35km North of Leuven). A correlation study with the measuring station of Heverlee, for which measurements are available until 2009, shows a good correlation between the temperatures of the two measuring points.

A similar investigation by Pedersen et al. (2010) on the LAWR radar (bigger version of the LAWR-CR) showed that the duration and the mean rainfall intensity had a significant impact on the radar-gauge deviations. These findings were checked for the LAWR-CR in its current setup and the analysis expanded with the other variables mentioned above.

- Convective- stratiform separation algorithm

The convective-stratiform separation algorithm (based on Steiner et al. 1995) looks for convective regions in the radar image by applying a two-step method. The first step simply applies a threshold value, originally around 42dBZ. All pixels above this threshold are categorized as convective centers and a region around these pixels as convective region. In the second step, the reflectivity of a certain pixel is compared to the surrounding region. If the reflectivity of the pixel fits a number of restraints and equations containing the reflectivity of the surrounding region, the pixel is also marked as a convective center with its convective surrounding region as in step 1. These two steps are a good representation of the physical reality of convective rainfall, where a strong convective center is surrounded by a convective region. It is generally acknowledged (among others in Houze, 1981; Caracciolo et al. 2006; Steiner et al. 1995 and the papers based on the latter) that above a certain threshold, there is nearly no stratiform rainfall present anymore, making the first step a good recognizing mechanism. The second step makes it possible to find convective centers below the threshold, while not easily confusing stratiform rainfall since this type of rainfall is known for its uniform horizontal structure.

- Cloud movement speed and direction determination algorithm

The cloud movement speed and direction determination algorithm compares two consecutive radar images to find the best cloud movement speed and direction at which the difference between the two images is minimized. For this, the algorithm first filters out the regions that the observed image and the proposed image have in common and then computes the RMSE of the difference in radar reflectivity values. This assumes that the cloud development takes place on a longer timescale than several minutes, so that the radar reflectivity values of two consecutive scans are similar. In this way, the best instantaneous cloud movement speed and direction can be obtained.

## 3. Results

### Influence of rain event type: convective versus stratiform events

No clear dependency could be found between the adjustment factor and the convective-stratiform type of rain event, at least for this particular radar-rain gauge configuration and the data periods investigated. For the WZ gauge, the adjustment factor is a bit higher for convective events in comparison with stratiform events, but relative magnitude difference is negligible. This does, however, not mean that the separation between convective and stratiform events is useless; it was found useful when studying other explanatory variables.

### Influence of the season

Summer (JJA) and autumn (SON) seasons give quite similar adjustment factor, whereas rain events during the winter season (DJF) have clearly a lower factor. For the spring season (MAM), a higher adjustment factor is found, indicating that the radar tends to underestimate events during spring. A possible explanation for this can be found in the section interlinking the seasonal and directional variances, where it is explained that the regression slope is lifted by a number of events.

Figure 3 (left) shows the group scatter plot of the different rain events (for the example rain gauge HB) separated into the different seasons, together with the linear regression results for each season. The uncertainty in the estimation of the regression slope is shown on the right-hand side of the figure, where the mean and 25% (Q1) and 75% (Q3) quartiles are shown, as well as the under and upper limit of the 95% confidence interval on the estimation of the regression slope.

The lower adjustment factor for the winter season is not surprising and could be the influence of the TBR's underestimating the actual rainfall depth or the radar overestimating the rainfall depth or both effects combined. A possible factor causing the underestimation of the rainfall depth by the TBR during winter could be the influence of snow and hail. Hail has a higher reflectivity, because of its bigger diameter. The same effect can take place if the precipitation consists of snowflakes, since they also have a bigger diameter than raindrops. The equation between the radar reflectivity Z [$mm^6/m^3$] and the drop size is, according to Battan (1973): $Z = \int_0^\infty D^6 N_V(D) dD$. Another factor starts to play a role when the outer layer of the hail or snow particle melts and its surface is covered by water. Such wet outer particle layer increases the reflectivity significantly, since the reflectivity of water is 5 times larger than the reflectivity of ice. These effects of reflectivity could seriously increase the measured DRO during the winter season. However, as there are not so many snow days during the measurement period, this is thought to be of less importance.

When the convective and stratiform events are analyzed separately, it is found that the convective events are present mostly during summer and autumn. There are only a limited number of convective storms present during winter and spring. The higher adjustment factor during spring and the lower one during winter are caused by stratiform events only. For autumn and summer, the adjustment factors of the convective and stratiform events are quite similar and no clear conclusions can be drawn.

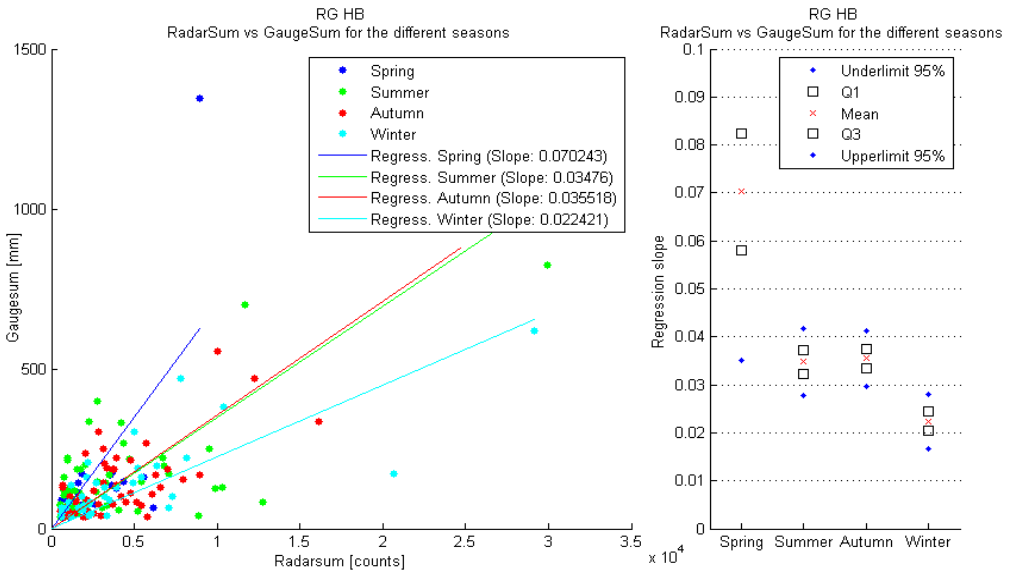


*Figure 3: (left) Scatter plot of Radarsum versus Gaugesum and linear regression for each season; (right) An alternative box plot for the regression slope (the mean regression slope is indicated, as well as the lower and upper quartiles and the lower and upper limits of the 95% confidence interval on the regression slope).*

Next to the influence of the rain event type per season, also the influence of cloud movement directions was studied. These directions are roughly divided in North, East, South and West. First of all, it should be mentioned that for the Belgian climate, the dominant cloud movement direction during each season is the westerly direction (more than 75% of all rain events). The easterly direction is the least present (less than 2.5% of all events). The relative and overall storm frequencies during the different seasons are shown in Table 3.

*Table 3: Frequency of occurrence of rain events during the different seasons and with different directions*

| | Direction | North | | East | | South | | West | |
|---|---|---|---|---|---|---|---|---|---|
| Season | Rel. Freq | Relative | Overall | Relative | Overall | Relative | Overall | Relative | Overall |
| Spring | 13.6% | 10% | 1.4% | 6% | 0.8% | 14% | 1.9% | 70% | 9.5% |
| Summer | 35.9% | 2% | 0.7% | 2% | 0.7% | 15% | 5.4% | 81% | 29.1% |
| Autumn | 30.4% | 18% | 5.5% | 2% | 0.6% | 10% | 3.0% | 70% | 21.3% |
| Winter | 20.1% | 25% | 5.0% | 0% | 0.0% | 0% | 0.0% | 75% | 15.1% |

The higher adjustment factor for the spring season cannot be explained by differences in the directional regression slopes. During spring, again, the westerly direction is most dominant (70%), whereas the northerly (relative occurrence 10%) and southerly (14%) directions are less frequent, even to the extent that the regression slope is highly uncertain due to the small number of events within each direction. The adjustment factor for the westerly direction is however a lot lower than the factor based on all cloud movement directions. The higher adjustment factors are found for the non-westerly events and for some westerly storms only. For the other seasons, the adjustment factor is a weighted combination of the factors obtained for each of the separate cloud movement directions.

**Influence of the cloud movement direction and speed**

The influence of the cloud movement direction is further investigated (Figure 4). Next to the low frequency of the easterly directions, there are nearly no easterly directions resulting in a rain event that passes the selection criteria. This is due to the fact that easterly winds are dry overland winds, which do not tend to carry along precipitating clouds. For the westerly and northerly directions, the adjustment factors are almost identical for all cases. The westerly's are by far the most present, which is not surprising as this directions caries along moist air from over the English Channel and the Atlantic Ocean. The storms with a southerly direction however have an adjustment factor that is higher than the slopes of the northerlies and Westerly's. A contributing factor to this difference is the low frequency of occurrence of southerly events during the winter period, where the northerly direction is more frequent, as can be seen in Table 3.

For the subdivision into classes of different cloud movement speeds, no clear and persistent relations could be found. In some cases, a slightly higher adjustment factor can be seen for the higher speeds. This is however not consistent for all the gauges and time periods.

The different cloud movement directions were further separated in subclasses based on the cloud movement speed. For the easterly direction, the number of rain events per class were too limited to allow a meaningful analysis. Also for the southern direction, the number of events per class were very limited. The northern direction does not show much difference of the adjustment factor with varying cloud movement speed, although it must be mentioned that the cloud movement speed does not vary that much for the northern direction. For the western direction, however, the adjustment factor shows an increasing value with increasing cloud movement speeds (Figure 5).

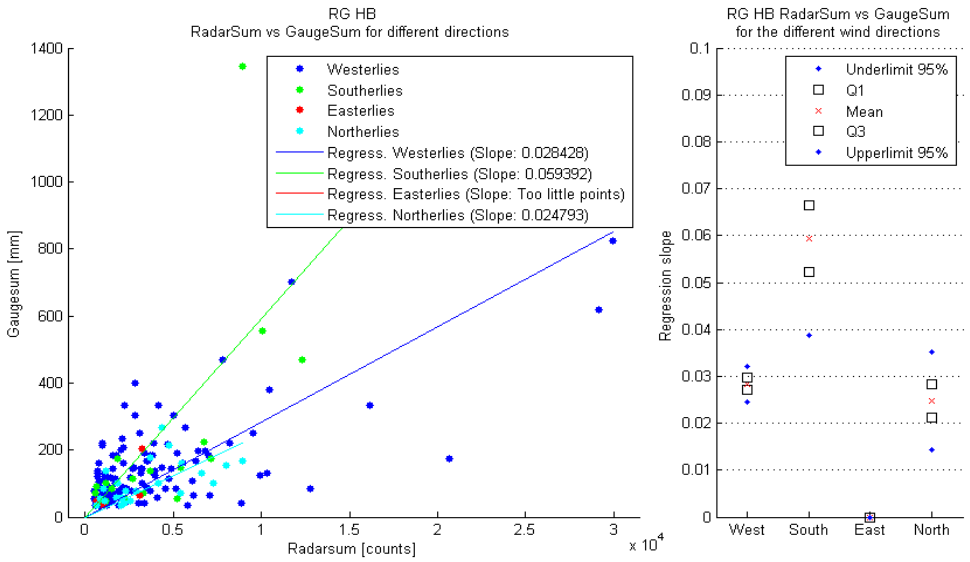


*Figure 4: (left) Scatter plot of Radarsum versus Gaugesum and linear regression for each direction; (right) An alternative box plot for the regression slope (the mean regression slope is indicated, as well as the lower and upper quartiles and the lower and upper limits of the 95% confidence interval on the regression slope).*

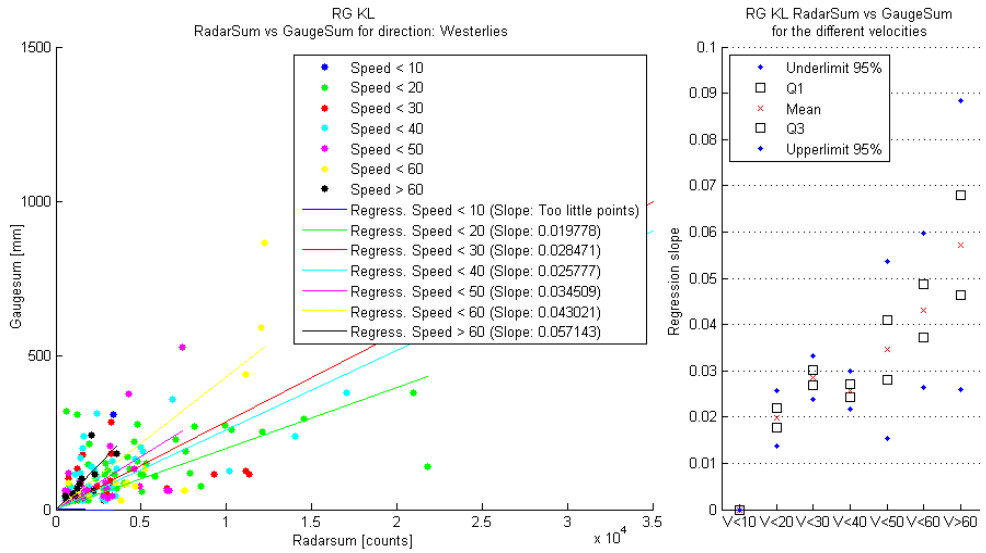


*Figure 5: (left) Scatter plot of Radarsum versus Gaugesum for each speed group; (right) An alternative box plot for the regression slope (the mean regression slope is indicated, as well as the lower and upper quartiles and the lower and upper limits of the 95% confidence interval on the regression slope).*

**Influence of the event duration**

For the duration of the events, a slightly higher adjustment factor is found for durations shorter than an hour. For other duration classes, no clear trends could be found. The higher relation for the shorter events could be due to intense isolated short lasting convective cells passing over the Leuven area. These events however only contain a small number of counts and a small amount of rain. They are thus less relevant in urban drainage studies.

**Influence of the spatial rain coverage of the radar image**

The spatial rain coverage is defined as the relative filling of the radar image where a signal above a certain threshold is found. This threshold is set to a low value to cut off clutter areas but not genuine rain. For a spatial coverage between 40 and 50%, a higher adjustment factor is found. No clear explanation for this has been found, but apparently clouds systems with this size precipitate more for the same amount of measured reflectivity. For the other spatial coverage classes, the adjustment factor is lower and more consistent over the different classes.

When the convective and stratiform events are analyzed separately per spatial coverage class, it is seen that convective events generally have a smaller spatial coverage (until 40%). Stratiform events cover a wider range of different spatial coverage classes. The higher adjustment factor for spatial coverage percentages between 40 and 50% is thus caused by stratiform events only.

**Influence of the air temperature**

The influence of the mean air temperature during the event is investigated, for temperatures lower than 10°C, a lower adjustment factor is found. For temperatures between 10°C and 20°C, a higher adjustment factor is found. There is thus

evidence of an increasing relationship with the temperature, but this relation is topped off at the highest temperatures. Also the correlation between the temperature and the convective or stratiform nature of the event is studied. The convective events generally correspond to mean air temperatures higher than 10°C. The stratiform events have a wider temperature range.

The lower adjustment factor for low temperatures is not surprising. These events occur in the winter season, for which the adjustment factor was found lower as well. For temperatures between 10° and 20°, most of the events causing the higher adjustment factor occur during the spring season, for which a higher factor was found. The events above 20°C almost all occurred during the summer season, for which the influence was a bit lower than the spring season.

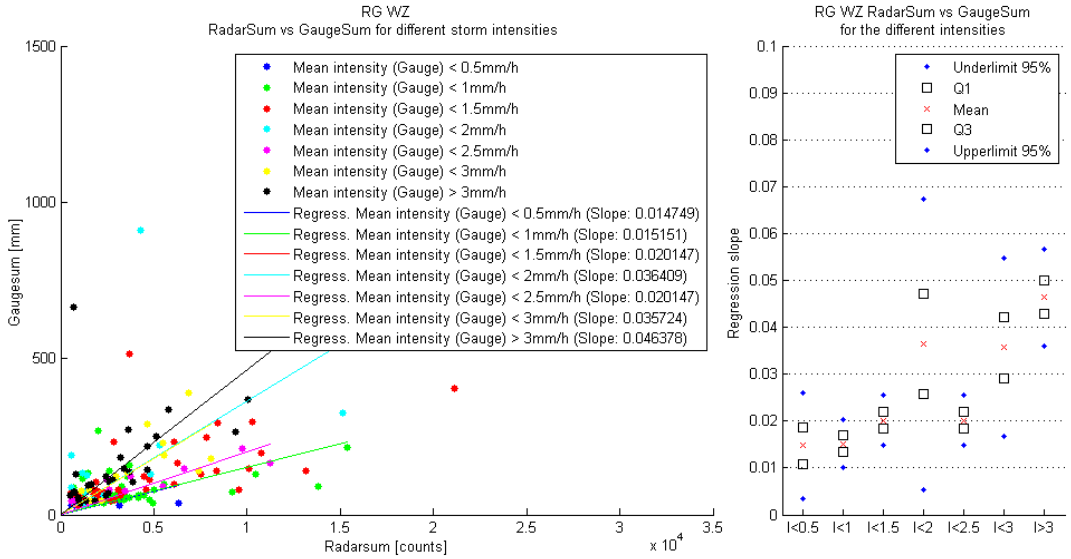


*Figure 6: (left) Scatter plot of Radarsum versus Gaugesum and linear regression for each intensity group; (right) An alternative box plot for the regression slope (the mean regression slope is indicated, as well as the lower and upper quartiles and the lower and upper limits of the 95% confidence interval on the regression slope).*

### Influence of the mean rainfall intensity

For the entire dataset, an increasing adjustment factor can be found with increasing mean rainfall intensity during the event, as measured by the rain gauges. The influence is quite clear (Figure 6). The positive influence means that for an equal amount of precipitation measured by the gauges, a lower radar reading will be found for more intense events, resulting in an underestimation of the total rainfall amount if this difference is not taken into account. If the seasonal variance is taken into account, it is noticeable that during the winter and spring seasons there are very limited number of storms with high-mean rainfall intensities. During summer and autumn seasons however, the influence is more prominent.

## 3. Conclusions

A new radar rainfall adjustment procedure has been developed and tested, based on variables that were found to influence the radar-gauge differences. These variables are the mean rainfall intensity (based on the gauges), the seasonal variance, the directional variance, for the westerly direction also the dependency of the cloud movement speed and possibly the relative rain coverage of the radar image.

## Acknowledgment

This research got financial support from the INTERREG IVb project RainGain (www.raingain.eu), the project for the Fund for Scientific Research (F.W.O.-Flanders) and the PLURISK project for the Belgian Science Policy Office. The authors would also like to thank Aquafin for funding the previous research project by T. Goormans and for keeping the radar operational for the RainGain project. They acknowledge also the Province of Flemish Brabant for allowing the installation of the LAWR-CR on its property. Rain gauge and temperature data were provided by Aquafin and the Flemish Environment Agency (VMM)

## References

Battan L.J., 1973: Radar observations of the atmosphere. University of Chicago Press.

Caracciolo C., Prodi F., Battaglia A., Porcu F., 2006: Analysis of the moments and parameters of a gamma DSD to infer precipitation properties: A convective stratiform discrimination algorithm. *Atmospheric Research*, **80**,165-186.

DHI, 2010: Local Area Weather Radar (LAWR) Documentation. Version 3.2, 1-49.

Goormans T., Willems P., 2008: Correcting rain gauge measurements for calibration of an X-band weather radar, Edinburgh, Scotland, UK: 11th International Conference on Urban Drainage.

Goormans T., 2011: Analysis of local weather radar data in support of sewer system modelling. PhD Thesis, Hydraulics Laboratory, KU Leuven, 2011, 220.

Houze, R.A.Jr. 1981: Structures of atmospheric precipitation systems: A global survey. *Radio Science*, **18**, 671-689.

Pedersen L., Jensen N.E., Madsen H., 2010: Calibration of Local Area Weather Radar - Identifying significant factors affecting the calibration. *Atmospheric Research*, **97**, 129–143.

Steiner M., Houze R.A., Yuter S.E., 1995: Climatological characterization of three-dimensional strom structure from operational radar and rain gauge data. *Journal of applied meteorology*, **34**, 1978-2007